Formation of dimethylketene and methacrolein by reaction of the CH radical with acetone

Fabien Goulay
West Virginia University, Fabien.goulay@mail.wvu.edu

Adeeb Derakhshan
West Virginia University

Eamonn Maher
West Virginia University

Adam J. Trevitt
University of Wollongong, adamt@uow.edu.au

John D. Savee
Sandia National Laboratories,Combustion Research Facility

See next page for additional authors

Recommended Citation

Formation of dimethylketene and methacrolein by reaction of the CH radical with acetone

Abstract

The reaction of the methylidyne radical (CH) with acetone ((CH3)2CO) is studied at room temperature and at a pressure of 4 Torr (533.3 Pa) using a multiplexed photoionization mass spectrometer coupled to the tunable vacuum ultraviolet synchrotron radiation of the Advanced Light Source at Lawrence Berkeley National Laboratory. The CH radicals are generated by 248 nm multiphoton photolysis of bromoform and react with acetone in an excess of helium and nitrogen gas flow. The main observed reaction exit channel is elimination of a hydrogen atom to form C4H6O isomers. Analysis of photoionization spectra identifies dimethylketene and methacrolein as the only H-elimination products. The best fit to the data gives branching ratios of 0.68 ± 0.14 for methacrolein and 0.32 ± 0.07 for dimethylketene. A methylketene spectrum measured here is used to reanalyze the photoionization spectrum obtained at m/z = 56 for the CH + acetaldehyde reaction, (Goulay et al., J. Phys. Chem. A, 2012, 116, 6091) yielding new H-loss branching ratios of 0.61 ± 0.12 for acrolein and 0.39 ± 0.08 for methylketene. The contribution from methyleneoxirane to the reaction product distribution is revised to be negligible. Coupled with additional product detection for the CD + acetone reaction, these observations pave the way for development of general set of reaction mechanisms for the addition of CH to compounds containing an acetyl subgroup.

Keywords

radical, ch, reaction, methacrolein, acetone, dimethylketene, formation, GeoQuest

Disciplines

Medicine and Health Sciences | Social and Behavioral Sciences

Authors

Fabien Goulay, Adeeb Derakhshan, Eamonn Maher, Adam J. Trevitt, John D. Savee, Adam M. Scheer, David L. Osborn, and Craig A. Taatjes

PCCP

RSCPublishing

PAPER

Formation of dimethylketene and methacrolein by reaction of the CH radical with acetone†

Fabien Goulay,*[a] Adeeb Derakhshan,[a] Eamonn Maher,[a] Adam J. Trevitt,[b] John D. Savee,[c] Adam M. Scheer,[c] David L. Osborn[c] and Craig A. Taatjes[c]

The reaction of the methylidyne radical (CH) with acetone ($(CH_3)_2C=O$) is studied at room temperature and at a pressure of 4 Torr (533.3 Pa) using a multiplexed photoionization mass spectrometer coupled to the tunable vacuum ultraviolet synchrotron radiation of the Advanced Light Source at Lawrence Berkeley National Laboratory. The CH radicals are generated by 248 nm multiphoton photolysis of bromoform and react with acetone in an excess of helium and nitrogen gas flow. The main observed reaction exit channel is elimination of a hydrogen atom to form C_4H_6O isomers. Analysis of photoionization spectra identifies dimethylketene and methacrolein as the only H-elimination products. The best fit to the data gives branching ratios of 0.68 ± 0.14 for methacrolein and 0.32 ± 0.07 for dimethylketene. A methylketene spectrum measured here is used to reanalyze the photoionization spectrum obtained at $m/z = 56$ for the CH + acetaldehyde reaction, (Goulay *et al.*, *J. Phys. Chem. A*, 2012, **116**, 6091) yielding new H-loss branching ratios of 0.61 ± 0.12 for acrolein and 0.39 ± 0.08 for methylketene. The contribution from methyleneoxirane to the reaction product distribution is revised to be negligible. Coupled with additional product detection for the CD + acetone reaction, these observations pave the way for development of general set of reaction mechanisms for the addition of CH to compounds containing an acetyl subgroup.

1. Introduction

With diminishing petrochemical resources and increasing concern about greenhouse gas emissions, biomass has emerged as a promising alternative source of liquid fuels.[1,2] Because biomass results from photosynthetic consumption of atmospheric CO_2, combustion of biomass-derived fuels is, in principle, a carbon-neutral process. Rapid transition to the use of biomass as a "carbon neutral" source of energy requires the adaptation of preexisting energy production infrastructure as well as a better understanding of the fundamental chemistry associated with biomass conversion. Thermochemical conversion of biomass generates a complex mixture that includes organic functional groups such as ketones, carboxylic acids, aldehydes, ketenes and cyclic ethers.[3–6] Despite their critical importance, mechanistic trends for the reaction of these primary products with combustion relevant radicals have not yet been fully developed.

The methylidyne (CH) radical has been detected in combustion flames[7,8] and is expected to play a significant role during the high-temperature processing of biomass-derived fuels. In a recent work, Goulay *et al.*[9] investigated the CH + acetaldehyde reaction in order to obtain general mechanistic information about the reactivity of CH radicals with aldehydes. The primary reaction product channels are formation of methylketene ($CH_3CH=C=O$) and acrolein ($H_2C=CHCH=O$). Ketene ($H_2C=C=O$) and the acetyl radical (CH_3CO) are also observed. The most likely methylketene formation mechanism from CH + acetaldehyde is cycloaddition of the radical onto the carbonyl group to form a cyclic intermediate that isomerizes by ring opening and loss of the hydrogen atom initially carried by the CH radical. Acrolein ($H_2C=CHCH=O$) is formed by the same addition mechanism followed by elimination of an H-atom initially from the methyl group of acetaldehyde. Methylene oxirane ($c\text{-}H_2C=COCH_2$) may also contribute to the product distribution but no reaction mechanism was proposed for its formation.

To investigate if the mechanistic trends determined for CH + acetaldehyde continue for ketones, the reaction of CH with the

[a] *Department of Chemistry, West Virginia University, Morgantown, West Virginia 26506, USA. E-mail: Fabien.goulay@mail.wvu.edu*
[b] *School of Chemistry, University of Wollongong, Wollongong, NSW 2522, Australia*
[c] *Combustion Research Facility, Mail Stop 9055, Sandia National Laboratories, Livermore, California 94551, USA*

† Electronic supplementary information (ESI) available. See DOI: 10.1039/c3cp43829e

smallest ketone, acetone ($CH_3(C{=}O)CH_3$) was studied. If an analogous mechanism is operative, the CH + acetone reaction will be a source of dimethylketene (($CH_3)_2C{=}C{=}O$) and methacrolein ($H_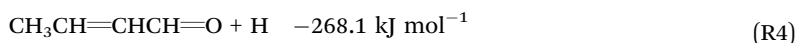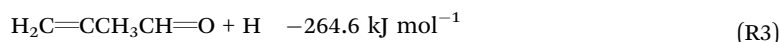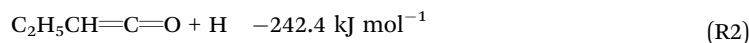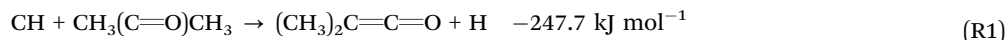2C{=}CCH_3CH{=}O$). Both dimethylketene and ethylketene ($C_2H_5CH{=}C{=}O$) are detected in ester flames.[10] Other C_4H_6O isomers include methyl vinyl ketone ($H_2C{=}CH(CO)CH_3$) and 2-butenal ($CH_3CH{=}CHCH{=}O$); all are identified as final products of glucose pyrolysis.[11] The likely thermodynamically favorable channels for the CH + acetone reaction are:

$$CH + CH_3(C{=}O)CH_3 \rightarrow (CH_3)_2C{=}C{=}O + H \quad -247.7 \text{ kJ mol}^{-1} \tag{R1}$$

$$C_2H_5CH{=}C{=}O + H \quad -242.4 \text{ kJ mol}^{-1} \tag{R2}$$

$$H_2C{=}CCH_3CH{=}O + H \quad -264.6 \text{ kJ mol}^{-1} \tag{R3}$$

$$CH_3CH{=}CHCH{=}O + H \quad -268.1 \text{ kJ mol}^{-1} \tag{R4}$$

$$H_2C{=}CHCCH_3{=}O + H \quad -273.2 \text{ kJ mol}^{-1} \tag{R5}$$
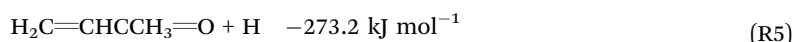
The enthalpies of reaction (at 298 K) are calculated using the enthalpy of formation of acetone,[12] methylidyne radical,[13] dimethylketene,[12] methacrolein,[14] 2-butenal,[14] and methyl vinyl ketone.[15] The heat of formation of ethylketene has not been experimentally determined and the enthalpy of reaction for the associated channel is calculated using the CBS-QB3 composite method[16] implemented within the Gaussian09[17] suite of programs.

In the present manuscript we report on the products of the CH/CD + acetone reaction. The experiments are performed utilizing a slow flow reactor coupled to a multiplexed photoionization mass spectrometer that uses tunable synchrotron radiation. In order to identify the isomeric structure of the products, we have synthesized and recorded the photoionization spectrum of ketene, methylketene, dimethylketene and ethylketene. By comparing the spectra of the pure compounds to the reaction products we identify dimethylketene and methacrolein as the only H-elimination products. The spectra of the synthesized ketene molecules are also used to reinvestigate the product distribution from the CH + acetaldehyde reaction. Finally, we propose a general reaction mechanism for the formation of ketenes and conjugated enal molecules by reaction of the CH radical with molecules containing an acetyl group ($CH_3C{=}O$).

2. Experimental section

2.1. Apparatus

A description of the apparatus is given elsewhere,[18–20] and only a brief overview is presented here. The gas flow consists of small amounts of bromoform and acetone in a large excess of helium and nitrogen buffer gas at a total pressure of 4 Torr (533.3 Pa) and at room temperature (total number density of $1.3 \times 10^{17} \text{ cm}^{-3}$). Prior to the experiment, a 5% gas mixture of acetone in helium is prepared in a 3.79 L stainless steel cylinder at a total pressure of 2000 Torr (2.668×10^5 Pa). A flow of He bubbles through liquid bromoform (at 8 °C) at a constant total pressure of 725 Torr (96.4×10^3 Pa). The total gas flow rate of 100 cubic-centimeters per minute (sccm) is obtained by mixing 1 sccm of the acetone–helium mixture, 2 sccm of the bromoform–helium mixture, 15 sccm of nitrogen and 82 sccm of helium.

The number densities of bromoform and acetone in the gas flow are $7.2 \times 10^{12} \text{ cm}^{-3}$ and $1.3 \times 10^{14} \text{ cm}^{-3}$, respectively. The sample of deuterated bromoform is prepared in the same manner. The purities of gases and reactants are as follows: He, 99.9999%; bromoform, >99%; D-bromoform, 99.5 atom% D, with 1% carbon tetrabromide; acetone, 99.9%.

The CH radicals are produced coaxially in the flow by 248 nm multiphoton photolysis of bromoform using the unfocused beam of an excimer laser with a 4 Hz repetition rate and a laser fluence between 50 mJ cm^{-2} and 75 mJ cm^{-2}. The number density of nitrogen in the flow ($1.93 \times 10^{16} \text{ cm}^{-3}$) is sufficient to rapidly quench any vibrationally excited CH radicals formed during the photolysis of bromoform.[21–23] The chemical reaction proceeds uniformly along the length of the reactor as the irradiated gas moves through the tube. The gas flow is sampled through a $\sim$650 μm diameter pinhole into a low pressure chamber (typically 1.3×10^{-3} Pa). The nearly effusive beam is then passed through a 1.5 mm diameter skimmer before entering a differentially pumped ionization region. The gas beam is crossed by vacuum ultraviolet (VUV) synchrotron undulator radiation that is dispersed by a 3 m monochromator at the Chemical Dynamics Beamline[24] of the Advanced Light Source at Lawrence Berkeley National Laboratory. All masses of resulting ions are monitored at 50 kHz using an orthogonal accelerated time-of-flight mass spectrometer equipped with a time-sensitive microchannel plate detector. The experiment is repeated for 250 to 5000 photolysis laser pulses, and the data are summed. Background signals corresponding to a pre-photolysis signal averaged over 20 ms are subtracted. The background-subtracted signals are normalized for the VUV photon flux at each photon energy. Photoionization spectra are then constructed by integrating the three-dimensional data set first over

4050 | Phys. Chem. Chem. Phys., 2013, 15, 4049–4058

This journal is © the Owner Societies 2013

Table 1 Anhydride precursors, mantle and the trap temperatures used for the synthesis of the ketene derivatives

Molecules	Precursor	Heating mantle temperature (°C)	Temperature of the first trap (°C)	Temperature of the second trap (°C)
Ketene	Acetic anhydride	163	−41	−196
Methylketene	Propionic anhydride	200	−41	−196
Ethylketene	Butyric anhydride	230	−63	−196
Dimethylketene	Isobutyric anhydride	210	−63	−196

the desired mass-to-charge ratio then over an appropriate time window. Three independent datasets are recorded for each reaction. The photoionization spectra from each dataset are normalized by the area under the curve and averaged. The error bars at a given photon energy are twice the standard deviation around the mean of the three measurements. The photon energy and the energy resolution (~ 40 meV for 600 μm exit slit width) are determined by measurement of known atomic resonances of Xe.

2.2. Synthesis and photoionization spectrum of ketene and ketene derivatives

Ketene, methylketene, dimethylketene and ethylketene were synthesized using variations to the procedure reported by Williams and Hurd.[25] A full description of ketene synthesis is given by Yang et al.[26] and only a brief overview is given here. Table 1 presents a list of the anhydride precursors and the trap temperatures used for each ketene derivative. About 50 to 100 mL of the anhydride precursor is refluxed under flowing nitrogen at atmospheric pressure. A nichrome coil inserted into the reaction flask is resistively heated to a dull red glow at a temperature sufficient to crack the anhydride. The mixture of gaseous products travels through a water-cooled condenser into a first cold trap. The desired volatile ketene product is then collected at 77 K in a large glass bubbler. Any highly volatile impurities in the final trap are removed by thawing and pumping off 10 to 20% of the condensed sample. After removing the nitrogen from the glass vessel, 20 Torr of the ketene derivative and 980 Torr of helium were combined in a 3.79 L stainless steel cylinder. Photoionization spectra of each individual ketene derivative are measured by flowing 1 sccm of the $\sim 2\%$ ketene in He mixture with 1 sccm of a $\sim 0.4\%$ propene or $\sim 1\%$ 1-butene (as internal standards) in He mixture and 98 sccm of additional He. The total pressure in the reaction flow tube is maintained at 4 Torr.

3. Results

The laser dissociation of bromoform is known to produce $CHBr_2$, $CHBr$, CH as well as Br and Br_2.[27] Both the reactions of the doublet CH and the singlet CHBr can give rise to products at $m/z = 70$, by loss of H and HBr, respectively. Previous experimental studies however, report a very low yield for the formation of CHBr at 248 nm compared to 193 nm photodissociation.[27,28] At 193 nm, CHBr is formed by single-photon dissociation with a cross section of 3.42×10^{-18} cm^2 and a yield of 0.3.[27,29] At 248 nm the formation of CHBr was reported to be below the detection limit using transient spectroscopy, which suggested that its number density is at least 200 times less than at 193 nm.[27] For a 248 nm laser fluence of 50 mJ cm^{-2} this corresponds to a CHBr number density

at least 5 times lower than the CH number density estimated using the formula of Romanzin et al.[30] At 193 or 266 nm, however, the number density of CHBr is expected to be much greater than that of CH.[7]

The CHBr singlet carbene can react with acetone to form a cyclic intermediate. The two most likely product channels in this reaction are the stabilization of the initial adduct to form a product at $m/z = 150$ and 152, or HBr loss to form a cyclic carbene that may in turn isomerize to dimethylketene. Ring opening of the initial intermediate to form a diradical or 1, 3 H–Br elimination to form methacrolein seems far less likely. In any case, the observation of $m/z = 150$ and 152 implies that the branching ratio for formation of $m/z = 70$ products via HBr loss is less than unity. Combined with the low relative number density of CHBr this suggests that the contribution from the CHBr + acetone reaction to the $m/z = 70$ products is relatively small and is within the branching ratio estimated errors.

In the following section, we analyze mass spectra and photoionization spectra corresponding to the products of the reactions of the CH and CD radicals with acetone. When analyzing the photoionization spectra, within the experimental energy resolution we neglect the effect of isotope substitution on the ionization energy and ionization cross-section.[31] The isomeric structures of the reaction products are identified by comparing their photoionization spectra to that of pure standards, either commercially available or synthesized. The contribution from the single and two-photon dissociation of acetone at 248 nm is determined by recording the photoionization spectrum in identical experimental conditions but excluding bromoform.

3.1. Photoionization spectra of the ketene molecules

Fig. 1 displays the photoionization spectra of the synthetized ketene derivatives (a) relative to the known absolute photoionization spectrum of propene[32] or 1-butene and (b) normalized to the photoionization cross-section of ketene. All spectra display a strong photoionization shape resonance peaking between 10.0 and 10.2 eV. The absolute photoionization spectrum of ketene compares very well with the one published by Yang et al.[26] In Fig. 1(a) the value of the methylketene photoionization cross section at 11.5 eV is one third that of dimethylketene at the same energy. According to the semi-empirical model of Bobeldijk et al.[33] the substitution of a hydrogen atom by a methyl group should increase the cross section of the continuum ionization at 11.5 eV, although this model is likely to be applicable only to cross-sections dominated by direct ionization processes. Moreover, unlike the series of acetylenes studied by Xu et al.,[34] methyl substitution of ketene does not significantly impact the wavefunction character for the frontier orbitals (see ESI†). Furthermore, none of the normally
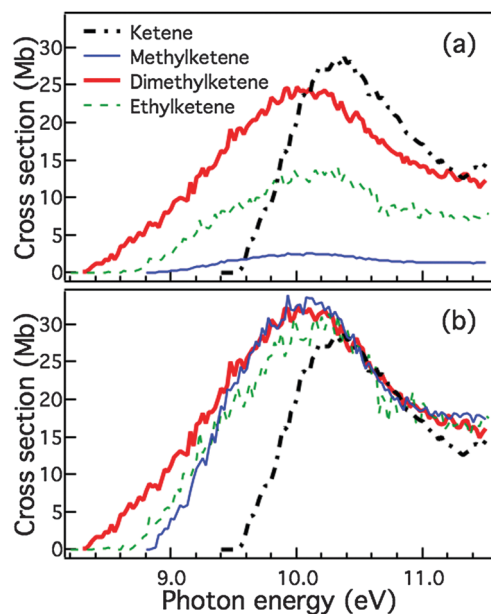
Fig. 1 Absolute photoionization spectrum of ketene (m/z = 42, dash-dotted black line), methylketene (m/z = 56, blue thin line), ethylketene (m/z = 70, green dashed line) and dimethylketene (m/z = 70, red line). The spectra in (a) are obtained by normalizing the raw spectra to the absolute spectra of propene or 1-butene introduced in the flow tube with the ketene molecules. The dispersion in absolute cross section for the substituted ketenes is likely to be due to polymerization or reaction of the ketenes on the tank walls. The spectra in (b) are normalized to the spectrum of ketene in the 10.6–10.8 eV energy range.

unoccupied orbitals display the g-wave (l = 4) character that Xu *et al.* associated with very strong shape resonances. Hence no dramatic change in the shape resonance intensity is expected for the substituted ketenes. Assuming that the intensity of the shape resonance is similar for all the ketene molecules, we attribute the lower measured cross section of ethylketene and methylketene to errors in the initial molecule number density in the sample gas mixture. Such errors could result from reaction of the gaseous substituted ketenes with the storage cylinder walls or to polymerization. Nevertheless the shape of the photoionization spectrum is reliable. The cross-sections of the substituted ketene are therefore estimated by normalizing the average value of the photoionization spectrum to that of CH_2CO in the 10.6–10.8 eV energy range (see Fig. 1(b)). Savee *et al.*[35] make a similar approximation and estimate the photoionization of methylketene by normalizing the spectrum to that of ketene in the energy range just after the maximum cross section.
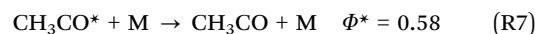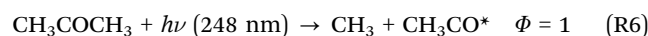
3.2. Acetone photodissociation

The photoabsorption cross-section of acetone at 248 nm is reported to be 2.2×10^{-20} cm^2.[36] The primary photodissociation products at 248 nm are the methyl (CH_3) and acetyl (CH_3CO) radicals.[37] The acetyl radical is formed with excess internal energy and can either be stabilized by collision with the buffer gas or dissociate to give CH_3 + CO.[37] Based on the study from Khamaganov *et al.*[37] the single-photon dissociation
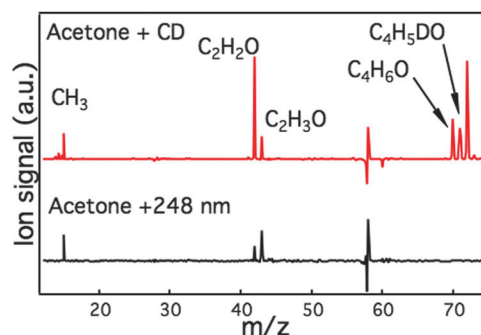
Fig. 2 Mass spectrum from the 248 nm photodissociation of acetone (lower black line) and the CD + acetone reaction (upper red line) integrated over the first 5 ms of reaction time and recorded at 10.2 eV.

mechanism and quantum yields Φ at 5 Torr in a buffer gas of nitrogen are as follows:

$$CH_3COCH_3 + h\nu \ (248 \ nm) \rightarrow CH_3 + CH_3CO^* \quad \Phi = 1 \quad (R6)$$

$$CH_3CO^* + M \rightarrow CH_3CO + M \quad \Phi^* = 0.58 \quad (R7)$$

$$CH_3CO^* \rightarrow CH_3 + CO \quad \Phi^* = 0.42 \quad (R8)$$

Although the ketene + CH_4 exit channel is exothermic at 248 nm its detection has not been previously reported. In our experiment, although the buffer gas is a mixture of helium and nitrogen, we assume the following overall quantum yields for dissociation of acetone at 248 nm: $\Phi(CH_3)$ = 1.42, $\Phi(CH_3CO)$ = 0.58 and $\Phi(CO)$ = 0.42. For an initial acetone density of 1.3×10^{14} cm^{-3} and for a 248 nm laser fluence of 70 mJ cm^{-2}, the densities of the acetone photoproducts immediately following photolysis are $[CH_3]_0 \approx 3.5 \times 10^{11}$ cm^{-3}, $[CH_3CO]_0 \approx 1.4 \times 10^{11}$ cm^{-3}, and $[CO]_0 \approx 1.0 \times 10^{11}$ cm^{-3}.

Fig. 2 displays the mass spectrum integrated from 0 to 5 ms for acetone photodissociation at 248 nm (black line) and the CD + acetone reaction (red line) recorded at 10.2 eV ionization energy. The signal at m/z = 58 is due to the background subtraction of the acetone peak. The main acetone photodissociation products are the methyl radical (CH_3) at m/z = 15 and ketene at m/z = 42. The small signal at m/z = 43 is likely to be due to the ionization of the acetyl radical (CH_3CO) produced by photodissociation of acetone and stabilized by collision with the helium and nitrogen buffer gases. Shin *et al.*[38] report the detection of H-atoms from the 243 nm dissociation of acetone. The translational energy of the observed H-atoms, measured by Doppler broadening, is found to be greater than the energy available after H-elimination from acetone (forming the acetonyl radical, CH_3CH_2CO). The authors propose a consecutive two-photon absorption mechanism during which the initially formed acetyl radicals can absorb a second photon providing sufficient energy to surmount the 262 kJ mol^{-1} energy barrier and dissociate to give ketene + H.[38] A similar consecutive two-photon absorption process has been proposed for the dissociation of bromoform to form CH radicals and may explain the observed ketene in our experiments conducted without bromoform.[30]

In the case of a one-photon process, the number densities of photodissociation products scale linearly with laser power. In the
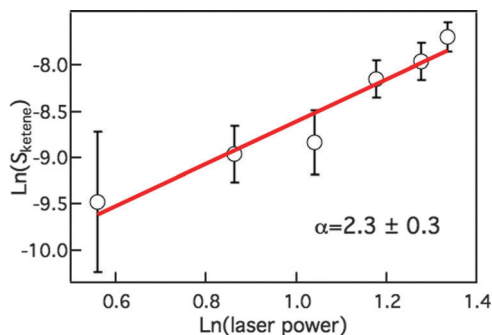
Fig. 3 Dependence of the ketene signal as a function of laser output power. The red line is a linear fit resulting in a slope $\alpha = 2.3 \pm 0.3$.

Fig. 5 Time traces of the ion signal at $m/z = $ (a) 42 and (b) 70 for the CH + acetone reaction and $m/z = $ (c) 70 and (d) 71 for the CD + acetone reaction integrated from 8.2 to 10.3 eV.
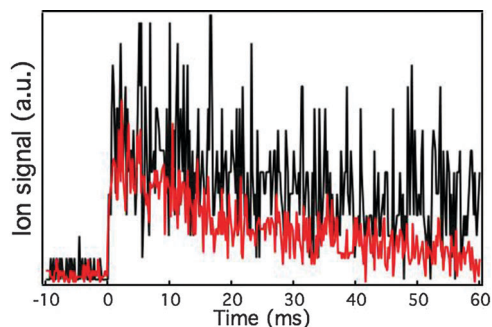
approximation of a small 248 nm absorption, the successive absorption of a second photon (during the same ~ 20 ns laser pulse) by the primary photoproducts leads to a quadratic dependence of the number densities of the final products with laser power. S_{ketene}, the measured signal of the ketene ions, is proportional to the number density and is obtained by fitting the time-resolved ion signal at 10.2 eV with a step function. The laser power is measured directly at the output of the laser using a calibrated thermopile and is proportional to the fluence in the reaction flow. The dependence of the ion signal with laser power can be written:

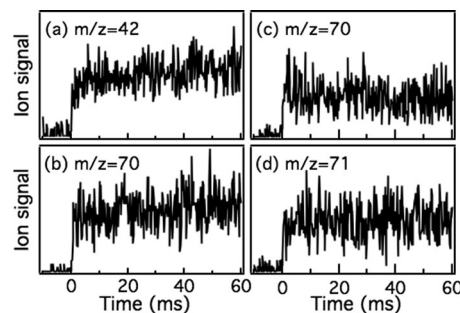$$\ln(S_{ketene}) = \ln(K) + \alpha \ln(Power) \qquad (1)$$

where K is a constant including the photoionization cross-sections of acetone and acetyl at 248 nm and the detector characteristic and α is the exponent describing the dependence of the ketene signal with laser power, with $\alpha = 1$ corresponding to one-photon absorption or $\alpha = 2$ corresponding to two-photon absorption). Fig. 3 displays the dependence of the logarithm of S_{ketene} as a function of the logarithm of the laser power. A linear fit gives $\alpha = 2.3 \pm 0.3$. The error bars represent one standard deviation from the fitting routine. This value is consistent with a two-photon formation process for ketene.

3.3. Reaction of CH/CD + acetone

Fig. 4 displays kinetic traces recorded at $m/z = 15$ (CH$_3$) and 10.2 eV for acetone photodissociation at 248 nm for pure


Fig. 4 Time traces of the ion signal at $m/z = 15$ for the dissociation of acetone at 248 nm (black line) and from the CD + acetone experiments (red line) recorded at 10.2 eV photon energy. The data are normalized by the total number of laser shots.

acetone (black line) and for acetone with d-bromoform (red line). The data are normalized by the total number of laser shots. No signal is observed at $m/z = 16$ (CH$_2$D). Up to 5 ms after the laser pulse, the rise time and intensity of the methyl radical signal are similar for both experiments. This suggests that CH$_3$ is produced as a direct photolytic product in both cases and not formed in any significant amount by the CH/CD + acetone reaction. Over a longer time frame, the CH$_3$ signal decays faster with bromoform than without it; this is likely due to the CH$_3$ + CDBr$_3$ secondary reaction. In the following sections we assume that all the CH$_3$ radicals are from acetone photodissociation and not a result of the CH/CD + acetone reaction. The CD + acetone mass spectrum recorded from 0 to 5 ms and displayed in Fig. 2 can therefore be normalized to the spectrum without bromoform at $m/z = 15$. In Fig. 2 the signal at $m/z = 43$ is the same in both spectra suggesting that the acetyl radical is not produced by the CH/CD + acetone reactions. Neglecting the acetone photoproducts, the main signals for the CH + acetone reaction appear at $m/z = 42$, 70 and 71 and at $m/z = 42$, 70, 71 and 72 for the CD + acetone reaction. For both reactions, only a small amount of the $m/z = 42$ signal can be attributed to acetone dissociation. Fig. 5 displays the kinetic traces of the ion signal at $m/z = $ (a) 42 and (b) 70 for the CH + acetone and $m/z = $ (c) 70 and (d) 71 for the CD + acetone reaction integrated from 8.2 to 10.3 eV. The signal at $m/z = 71$ (72 for the CD experiment) has an ionization energy onset of ~ 9.65 eV and may be due to either ionization of the stabilized C$_4$H$_7$O (C$_4$H$_6$DO) reaction adduct or to dissociative ionization of higher mass molecules that result from secondary chemistry. Stabilized C$_4$H$_7$O (C$_4$H$_6$DO) is expected to react with the excess acetone and bromoform in the reaction flow or heterogeneously with the walls of the quartz reactor. However, the kinetic trace of the $m/z = 71$ (72) cations shows no decay after the laser pulse and is therefore likely to come from the dissociative ionization of a stable closed shell molecule formed from secondary chemistry in the reaction flow. Two signals are detected at $m/z = 150$ (151) and $m/z = 152$ (153) with an ionization energy onset of ~ 8.85 eV. Both signals have the same intensity and do not decay over the entire reaction time. These ions are likely to originate from the ionization of C$_4$H$_7$OBr (C$_4$H$_6$DOBr) molecules formed by the CHBr (CDBr) + acetone and stabilization by the buffer gas. The dissociative ionization of these molecules at
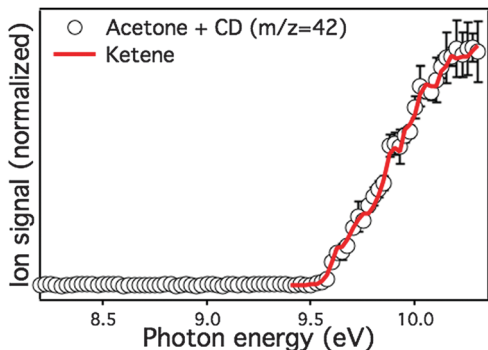
Fig. 6 Photoionization spectrum of $m/z = 42$ from the CD + acetone reaction. The solid line is the photoionization spectrum of ketene.

photon energies greater than 9.6 eV could form C_4H_7O (C_4H_6DO) cations at $m/z = 71$ (72) and Br atoms. The time traces of the brominated molecules and that of the $m/z = 71$ (72) signal are identical. Other brominated molecules formed after the laser pulse and identified by both their mass and ionization energy are vinyl bromide/d-vinyl bromide ($m/z = 107$ (108) and 109 (100), (AIE (adiabatic ionization energy) = 9.82 eV)[39] and isopropenyl bromide ($m/z = 121$, AIE = 9.58 eV),[40] non-deuterated for both CH and CD experiments.
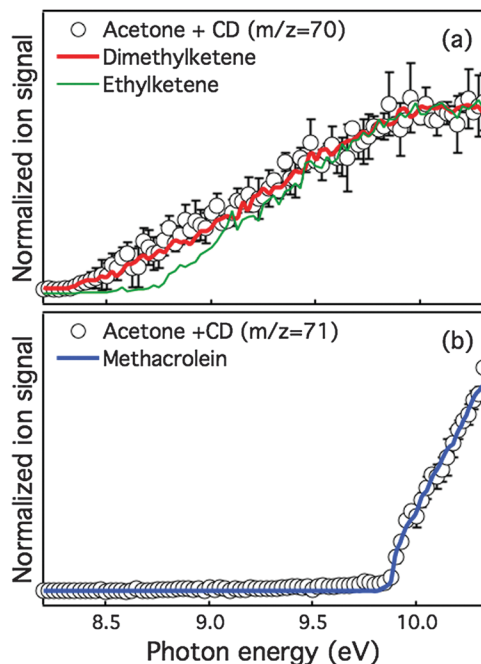
3.3.1. Ketene detection. Fig. 6 displays the photoionization spectrum at $m/z = 42$ from the CD + acetone reaction. The solid line is the known photoionization spectrum of ketene at $m/z = 42$. The very good match identifies ketene as the only isomer formed at $m/z = 42$. It is important to recall that only 14% of the ketene signal is from acetone photodissociation. In the case of the CD + acetone reaction we observe ketene at $m/z = 42$ and do not detect d-ketene at $m/z = 43$. The formation of ketene by the CH + acetone reaction is expected to be accompanied by the ethyl radical at $m/z = 29$ (AIE = 8.12 eV),[41] but no signal at this m/z value is detected here. The non-detection of the ethyl radical in the present experiment suggests that ketene is not formed by the CH + acetone reaction. A possible source of ketene is the hydrogen abstraction from the photolytically produced acetyl radical by hydrogen or Br atoms.
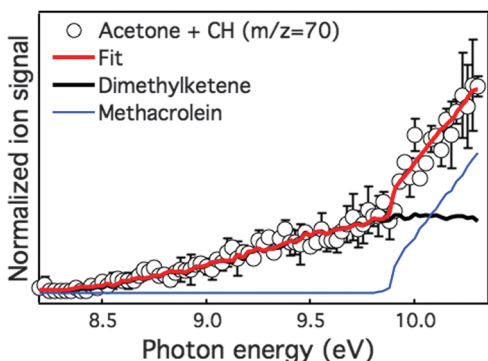
3.3.2. H/D-elimination channel. In the mass spectra presented in Fig. 2 the peaks at (a) $m/z = 70$ and (b) at $m/z = 70$ and 71 are assigned to ionization of the H-elimination products of CH + acetone. Fig. 7 displays the photoionization spectrum of $m/z = 70$ from the CH + acetone reaction integrated over the first 60 ms of reaction time. The spectrum displays two signal onsets that correspond to the ionization of dimethylketene at 8.38–8.45 eV[42,43] and methacrolein at 9.92 eV.[44] Below 9.8 eV the data can be fit by the photoionization spectrum of dimethylketene (black line). No ion signal onsets are observed near the ionization energies of either ethylketene (AIE = 8.80 eV)[42] or methyl vinyl ketone (AIE = 9.66 eV).[44] Over the entire experimental photon energy range the $m/z = 70$ data can be fit (red line) by a combination of the absolute photoionization spectra of dimethylketene and methacrolein (thin blue line). The photoionization spectrum of methacrolein was measured experimentally. Using the normalized photoionization spectrum for dimethylketene displayed in Fig. 1(b) the branching ratios are calculated to be 0.32 ± 0.07 dimethylketene and 0.68 ± 0.14 methacrolein. The estimated error is 20% of the branching ratio based on the uncertainty in the absolute cross-section of dimethylketene (described in Section 3.1).

Fig. 8 displays the photoionization spectra of (a) $m/z = 70$ (D-loss) and (b) $m/z = 71$ (H-loss) from the CD + acetone reaction. In Fig. 8(a) the thick red line is the absolute photoionization spectrum of dimethylketene and the thin green line that for ethylketene. The blue line in Fig. 8(b) is the absolute photoionization spectrum of methacrolein. The data can be well-fit

Fig. 7 Photoionization spectrum of $m/z = 70$ from the CH + acetone reaction. The thick red line is a fit to the experimental data including contributions from the absolute photoionization spectrum of dimethylketene (thick black line) and methacrolein (thin blue line).

Fig. 8 Photoionization spectrum of (a) $m/z = 70$ and (b) $m/z = 71$ from the CD + acetone reaction. The thick red line in panel (a) is a fit to the experimental data including only contribution from the photoionization spectrum of dimethylketene. The green line is the spectrum for ethylketene superposed on the experimental data. The blue line in panel (b) is a fit to the experimental data including only contribution from the photoionization spectrum of methacrolein.

4054 | Phys. Chem. Chem. Phys., 2013, **15**, 4049–4058

This journal is © the Owner Societies 2013

using the photoionization spectrum of dimethylketene to $m/z = 70$ and methacrolein to $m/z = 71$. In both cases the contributions from ethylketene or methyl vinyl ketone are negligible.

4. Discussion

From these experimental data, it is evident that the main CH + acetone reaction products are dimethylketene formed by elimination of the H-atom initially from the CH radical and methacrolein formed by elimination of a H-atom initially from a methyl group of acetone. Ketene is detected at $m/z = 42$ for both CH and CD reactions but because the expected C_2H_5 (C_2H_4D) co-products are not observed it is likely to be formed by side reactions. In the following section we discuss the possible CH/CD + acetone reaction mechanisms and compare them to the experimental isotopomer distributions. Coupled with previous results from the reaction of CH/CD with acetaldehyde, these observations pave the way for development of a general set of reaction mechanisms for the addition of CH to compounds containing an acetyl subgroup.

4.1. CH cyclo-addition to carbonyl group

Fig. 9 displays the proposed H-elimination reaction mechanism for the CH + acetone reaction. The hydrogen atom initially from the CH radical is labeled in bold. The CH radical can add to the carbonyl to form a cyclic intermediate reminiscent of the initial addition step in the CH + acetaldehyde reaction. Because we do not detect any cyclic final products, the direct elimination of a hydrogen atom from the cyclic intermediate is unlikely. Direct elimination of a methyl group would lead to methyl oxirene (c-CHOCCH$_3$) and a β-hydrogen transfer followed by elimination of a CH$_3$ radical would lead to methyleneoxirane (c-CH$_2$OC=CH$_2$),

both at $m/z = 56$. Because neither CH$_3$ ($m/z = 15$) nor signal at $m/z = 56$ are observed from the CH + acetone reaction, we deduce that the initial intermediate likely isomerizes by ring opening to form the (CH$_3$)$_2$CCHO radical (see Fig. 9). The resulting tertiary radical is generated with excess energy and direct H-elimination by loss of the H-atom initially from the CH radical gives dimethylketene ((CH$_3$)$_2$C=C=O). Alternatively, loss of an H-atom from either of the two methyl groups gives methacrolein. This reaction mechanism is consistent with the isotopomer distributions from CD + acetone presented in Fig. 8. The reaction mechanism displayed in Fig. 9 does not describe pathways that lead to the formation of ketene, ethylketene or methyl vinyl ketone.

4.2. CH insertion to C–H bond

Insertion of the CH radical into a C–H bond of a methyl group has been reported to occur in the reaction with alkanes and was suggested for the CH + acetaldehyde reaction.[9,45,46] Fig. 10 displays the reaction mechanism for CH insertion into a C–H bond of acetone. The resulting radical can directly decompose to form methyl vinyl ketone + H. In this case the ejected H atom originates from one of the methyl groups of acetone and would form deuterated methyl vinyl ketone from CD + acetone, which is not detected. Methyl transfer, a less likely mechanism, could form a CH$_3$–CH$_2$–CH$_2$–CO radical. The elimination of an H-atom from this radical would form deuterated ethylketene from CD + acetone. The fact that neither ethylketene nor methyl vinyl ketone are detected at $m/z = 71$ by the CD + acetone reaction reinforces the previous conclusion that dimethylketene is the only contribution to the ion signal displayed in Fig. 8(a). The C_3H_7 radical from a possible CO + C_3H_7 dissociation channel is not also observed.

4.3. General reaction mechanism of CH + acetyl group

The present results for the reaction of CH + acetone and past investigations of the reaction of CH + acetaldehyde provide evidence for general mechanistic insight into the reaction of the CH radical with compounds containing an acetyl functional group. However, observations made in the present work warrant a minor reinterpretation of past results on CH + acetaldehyde that will be discussed first.

For the reaction of CH + acetaldehyde, Goulay et al.[9] proposed that below the ionization energy of acrolein, the difference between the simulated spectrum and the photoionization spectrum of methylketene is due to the presence of methylenoxirane (AIE = 9.92 eV).[9] However, none of the proposed reaction mechanisms were able to explain the
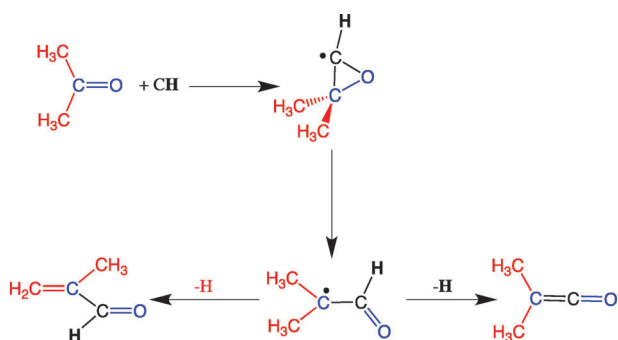
Fig. 9 Proposed reaction mechanism for the CH radical cycloaddition to acetone.

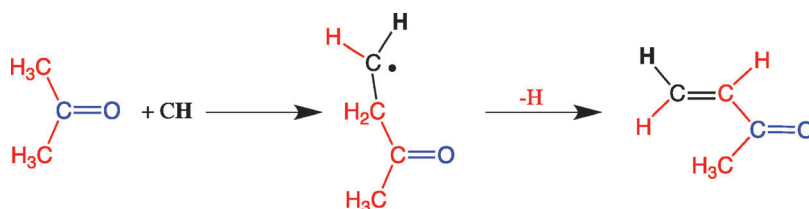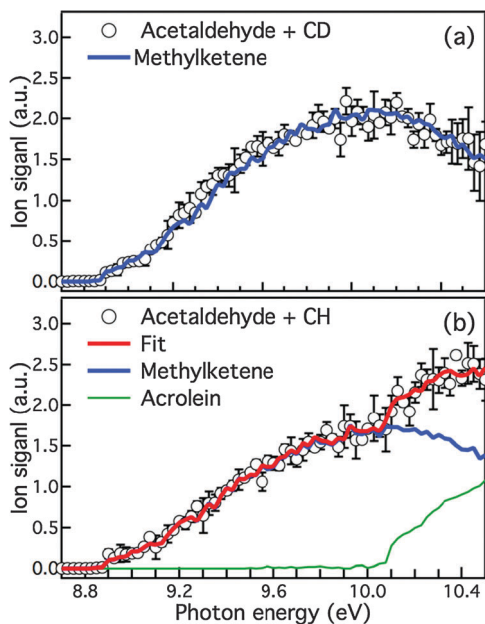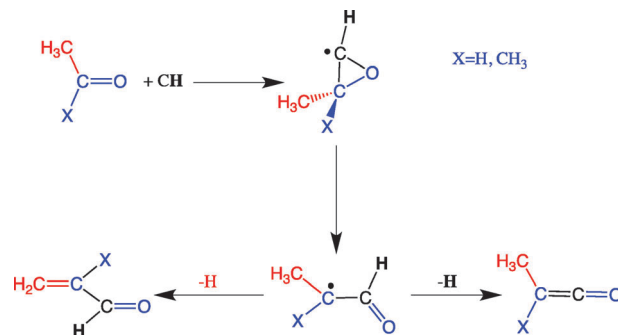**Fig. 10** Proposed reaction mechanism for the CH radical insertion into a C–H bond initially on one of the methyl groups of acetone.

Fig. 11 Photoionization spectrum of $m/z = 56$ from (a) CD + acetaldehyde and (b) CH + acetaldehyde. The blue line in both panels is the photoionization spectrum of methylketene fitted to the experimental data over (a) the entire energy range and (b) up to 10 eV. The red line in panel (b) is a fit to the experimental data including contribution from the photoionization spectrum of methylketene and acrolein (thin green line).

Fig. 12 Reaction mechanism for the CH radical cycloaddition to a molecule containing an acetyl functional group.

methylenoxirane isotopomer distribution. In light of the recently obtained experimental photoionization spectrum of methylketene, we reassign the CH (CD) + acetaldehyde $m/z = 56$ product channel. Fig. 11 displays the photoionization spectrum of $m/z = 56$ for (a) the CD + acetaldehyde reaction and (b) the CH + acetaldehyde reaction from ref. 10. The blue line in Fig. 11(a) is the photoionization spectrum of methylketene. The very good match between the two spectra suggests that methylketene is the only product formed by H-elimination from the CD + acetaldehyde reaction. The difference between the measured experimental spectrum of methylketene and simulated spectrum of the methylketene used previously[9] is likely due to the broad shape resonance[34] that is not predicted by the Franck–Condon simulation of continuum ionization. The conclusion from Goulay et al.[9] should be revised to remove the contribution from methyloxirane. It must also be noted that in a very recent work, Savee et al.[35] measured the photoionization spectrum of $m/z = 56$ from the O(^{3}P) + propene reaction. The spectrum is identical to the photoionization spectrum obtained at $m/z = 56$ from the CD + acetaldehyde reaction, and was seemingly correctly deduced as arising solely from methylketene.

The red line in Fig. 11(b) is a fit to the CH + acetaldehyde data using the absolute photoionization spectra of methylketene and acrolein only. The branching ratios for the CH + acetaldehyde reaction are calculated to be 0.39 ± 0.08 methylketene and 0.61 ± 0.12 acrolein. We report an error of $\pm 20\%$ of the branching ratio to reflect the uncertainty in the absolute cross-section of methylketene. The individual contribution from the spectra of methylketene (thick blue line) and acrolein

(thin green line) is also shown. Methylketene and acrolein are thus determined to be the only H-elimination products formed by the CH + acetaldehyde reaction. The CH cyclo-addition mechanism for CH + acetaldehyde proposed by Goulay et al. is consistent with this conclusion.

Fig. 12 presents a general reaction mechanism for the addition/H-elimination pathway for the CH + CH$_3$(C=O)X reaction. The CH radical adds to the carbonyl group to form a cyclic intermediate that directly isomerizes via ring-opening to form a resonance-stabilized substituted vinoxy-like radical. Dissociation of this intermediate forms a substituted ketene by elimination of the H-atom initially from the CH radical or a conjugated enal molecule by elimination of an H-atom initially from the methyl group. This reaction mechanism is validated experimentally for X = H (ref. 9) and X = CH$_3$ (present study), and may be applicable to larger ketones (X = C$_2$H$_5$, C$_3$H$_7$), enones (X = C$_2$H$_3$) and esters (X = OCH$_3$, OC$_2$H$_5$,...). In the case of esters, such a mechanism may be applicable to molecules containing long carbon chains like those found in biodiesels. The resulting substituted ketenes and conjugated enals are therefore likely to be important intermediates that will be present in the combustion of biofuels. In such environments substituted ketene molecules may react with themselves to form high mass dimers, thus contributing to molecular growth.

5. Conclusion

In the present work we have recorded time dependent photoionization spectra for the products of the CH and CD + acetone reactions. We have also synthesized and obtained photoionization spectra for methylketene, dimethylketene and ethylketene for isomer identification, which has aided not only the present investigation of CH/CD + acetone, but also led to a minor reinterpretation of results on the reaction of CH/CD + acetaldehyde. For the CH + acetone reaction, the photoionization spectra obtained at $m/z = 70$ reveal that dimethylketene and methacrolein are the sole H-elimination reaction products. Because of the large uncertainty in the concentration of the synthesized methyl substituted ketenes, their experimental peak cross-sections are normalized to that of ketene. The best fit to the reaction data gives branching ratios of 0.68 ± 0.14 for methacrolein and

0.32 $\pm$ 0.07 for dimethylketene. The normalized substituted ketene spectra are also used to reanalyze the photoionization spectrum obtained at $m/z = 56$ for the CH + acetaldehyde reaction,[9] yielding new H-loss branching ratios of 0.61 $\pm$ 0.12 for acrolein and 0.39 $\pm$ 0.08 for methylketene. The contribution from methyloxirane to the reaction product distribution is revised to be negligible. The detection of only methylketene by CD addition to acetaldehyde followed by D-elimination and of only acrolein by H-elimination agrees well with the cyclo-addition mechanism proposed by Goulay et al.[9]

For the CD + acetone reaction, dimethylketene is detected at $m/z = 70$ and methacrolein at $m/z = 71$. This suggests that the substituted ketene is formed by elimination of the D-atom initially from the methylidyne radical while methacrolein is formed by elimination of a H-atom from a methyl group of acetone. This isotopomer distribution suggests that the CH + acetaldehyde and CH + acetone reactions proceed via analogous reaction mechanisms. From these results, we propose a general mechanism for the CH reaction with ketones and aldehydes. The radical is likely to add to the C=O double bond to form an initial cyclic intermediate. Because we do not detect any cyclic products we infer that the most likely fate of this primary intermediate is isomerization by ring opening to form a resonance-stabilized substituted vinoxy radical. This intermediate is likely to be formed with a large amount of excess energy and can then decompose by losing a H-atom initially from the methyl group of the reactant molecule to form a conjugated enal or by losing the hydrogen atom initially from the radical to form a substituted ketene. Because all the transition states are likely to be well below the energy of the reactants, the mechanism is expected to be unchanged at higher temperatures. These reaction mechanisms are important in order to predict the fate of organic molecules in combustion environments. Theoretical validation of these mechanisms and further experiments on similar systems would be of considerable use in the validation of this general mechanism.

Acknowledgements

References

1 N. Z. Muradov and T. N. Veziroglu, *Int. J. Hydrogen Energy*, 2008, **33**, 6804–6839.

2 "National Hydrogen Energy Roadmap," U.S. Department of Energy, 2002.

3 T. Faravelli, A. Frassoldati, G. Migliavacca and E. Ranzi, *Biomass Bioenergy*, 2010, **34**, 290–301.

4 E. Ranzi, A. Cuoci, T. Faravelli, A. Frassoldati, G. Migliavacca, S. Pierucci and S. Sommariva, *Energy Fuels*, 2008, **22**, 4292–4300.

5 D. K. Shen and S. Gu, *Cellul. Chem. Technol.*, 2010, **44**, 79–87.

6 J. C. Kang, P. H. Chen and W. R. Johnson, Ketene formation from the pyrolysis of carbohydrates, in *Thermal uses and properties of carbohydrates and lignins*, ed. F. Shafizadeh, K. V. Sarkanen and D. A. Tillman, Academic press, New York, 1976, p. 261.

7 N. Love, R. N. Parthasarathy and S. R. Gollahalli, *Int. J. Green Energy*, 2011, **8**, 113–120.

8 F. V. Tinaut, M. Reyes, B. Gimenez and J. V. Pastor, *Energy Fuels*, 2011, **25**, 119–129.

9 F. Goulay, A. J. Trevitt, J. D. Savee, J. Bouwman, D. L. Osborn, C. A. Taatjes, K. R. Wilson and S. R. Leone, *J. Phys. Chem. A*, 2012, **116**, 6091–6106.

10 B. Yang, C. K. Westbrook, T. A. Cool, N. Hansen and K. Kohse-Hoinghaus, *Phys. Chem. Chem. Phys.*, 2011, **13**, 7205–7217.

11 Z. Zhan, Y. Lin, M. Pillai, I. Kim and S. A. Barnett, *J. Power Sources*, 2006, **161**, 460–465.

12 J. M. Simmie, W. K. Metcalfe and H. J. Curran, *Chem-PhysChem*, 2008, **9**, 700–702.

13 M. W. Chase, Jr., *J. Phys. Chem. Ref. Data, Monogr. 9*, 1998, **14**, 535, 1667.

14 Y. Y. Vanchinsyan, V. V. Kochubei, V. V. Sergeev, Y. A. Raevskii, S. I. Gerasimchuk and K. Z. Kotovich, *Zh. Fiz. Khim.*, 1996, **70**, 1932–1937.

15 J. P. Guthrie, *Can. J. Chem.*, 1978, **56**, 962–973.

16 J. W. Ochterski, G. A. Petersson and J. A. Montgomery, *J. Chem. Phys.*, 1996, **104**, 2598–2619.

17 M. J. Frisch, G. W. Trucks, H. B. Schlegel, G. E. Scuseria, M. A. Robb, J. R. Cheeseman, G. Scalmani, V. Barone, B. Mennucci, G. A. Petersson and H. Nakatsuji, et al., *Gaussian 09, Revision A.1*, Gaussian, Inc., Wallingford, CT.

18 S. Soorkia, C. A. Taatjes, D. L. Osborn, T. M. Selby, A. J. Trevitt, K. R. Wilson and S. R. Leone, *Phys. Chem. Chem. Phys.*, 2010, **12**, 8750–8758.

19 F. Goulay, D. L. Osborn, C. A. Taatjes, P. Zou, G. Meloni and S. R. Leone, *Phys. Chem. Chem. Phys.*, 2007, **9**, 4291–4300.

20 D. L. Osborn, P. Zou, H. Johnsen, C. C. Hayden, C. A. Taatjes, V. D. Knyazev, S. W. North, D. S. Peterka,

M. Ahmed and S. R. Leone, *Rev. Sci. Instrum.*, 2008, **79**, 104103.

21 L. B. Herbert, I. R. Sims, I. W. M. Smith, D. W. A. Stewart, A. Symonds, A. Canosa and B. R. Rowe, *J. Phys. Chem.*, 1996, **100**, 14928–14935.

22 F. Goulay, C. Rebrion-Rowe, L. Biennier, S. D. Le Picard, A. Canosa and B. R. Rowe, *J. Phys. Chem. A*, 2006, **110**, 3132–3137.

23 F. Goulay, A. J. Trevitt, G. Meloni, T. M. Selby, D. L. Osborn, C. A. Taatjes, L. Vereecken and S. R. Leone, *J. Am. Chem. Soc.*, 2009, **131**, 993–1005.

24 S. R. Leone, M. Ahmed and K. R. Wilson, *Phys. Chem. Chem. Phys.*, 2010, **12**, 6564–6578.

25 J. W. Williams and C. D. Hurd, *J. Org. Chem.*, 1940, **5**, 122–125.

26 B. Yang, J. Wang, T. A. Cool, N. Hansen, S. Skeen and D. L. Osborn, *Int. J. Mass Spectrom. Ion Processes*, 2012, **309**, 118–128.

27 P. Zou, J. N. Shu, T. J. Sears, G. E. Hall and S. W. North, *J. Phys. Chem. A*, 2004, **108**, 1482–1488.

28 B. C. Chang, J. Guss and T. J. Sears, *J. Mol. Spectrosc.*, 2003, **219**, 136–144.

29 B. C. Chang and T. J. Sears, *J. Chem. Phys.*, 1996, **105**, 2135–2140.

30 C. Romanzin, S. Boye-Peronne, D. Gauyacq, Y. Benilan, M. C. Gazeau and S. Douin, *J. Chem. Phys.*, 2006, **125**, 114312.

31 J. C. Person and P. P. Nicole, *J. Chem. Phys.*, 1970, **53**, 1767–1774.

32 O. Welz, J. D. Savee, D. L. Osborn, S. S. Vasu, C. J. Percival, D. E. Shallcross and C. A. Taatjes, *Science*, 2012, **335**, 204–207.

33 M. Bobeldijk, W. J. van der Zande and P. G. Kistemaker, *Chem. Phys.*, 1994, **179**, 125–130.

34 H. Xu, U. Jacovella, B. Ruscic, S. T. Pratt and R. R. Lucchese, *J. Chem. Phys.*, 2012, **136**, 154303.

35 J. D. Savee, O. Welz, C. A. Taatjes and D. L. Osborn, *Phys. Chem. Chem. Phys.*, 2012, **14**, 10410–10423.

36 T. Gierczak, J. B. Burkholder, S. Bauerle and A. R. Ravishankara, *Chem. Phys.*, 1998, **231**, 229–244.

37 V. Khamaganov, R. Karunanandan, A. Rodriguez and J. N. Crowley, *Phys. Chem. Chem. Phys.*, 2007, **9**, 4098–4113.

38 S. K. Shin, S. K. Kim, H. L. Kim and C. R. Park, *J. Photochem. Photobiol., A*, 2001, **143**, 11–16.

39 J. Momigny, *Nature*, 1963, **199**, 1179–1180.

40 D. Chadwick, D. C. Frost, A. Katrib, C. A. McDowell and R. A. N. McLean, *Can. J. Chem.*, 1972, **50**, 2642–2651.

41 B. Ruscic, J. Berkowitz, L. A. Curtiss and J. A. Pople, *J. Chem. Phys.*, 1989, **91**, 114–121.

42 H. Bock, T. Hirabayashi and S. Mohmand, *Chem. Ber./Recl.*, 1981, **114**, 2595–2608.

43 H. Bock, T. Hirabayashi, S. Mohmand and B. Solouki, *Angew. Chem., Int. Ed. Engl.*, 1977, **16**, 105–107.

44 P. Masclet and G. Mouvier, *J. Electron Spectrosc. Relat. Phenom.*, 1978, **14**, 77–97.

45 N. Galland, F. Caralp, Y. Hannachi, A. Bergeat and J. C. Loison, *J. Phys. Chem. A*, 2003, **107**, 5419–5426.

46 P. Fleurat-Lessard, J. C. Rayez, A. Bergeat and J. C. Loison, *Chem. Phys.*, 2002, **279**, 87–99.

4058 | *Phys. Chem. Chem. Phys.,* 2013, **15**, 4049–4058

This journal is © the Owner Societies 2013